



HAL
open science

Effects of hydrostatic pressure on amorphous chiral materials: Impact on homochiral or heterochiral H-bond sequences

Bienvenu Atawa, Nicolas Couvrat, Frederic Affouard, Natália Correia, Gérard Coquerel, Allisson Saiter-Fourcin

► To cite this version:

Bienvenu Atawa, Nicolas Couvrat, Frederic Affouard, Natália Correia, Gérard Coquerel, et al.. Effects of hydrostatic pressure on amorphous chiral materials: Impact on homochiral or heterochiral H-bond sequences. *Journal of Non-Crystalline Solids*, 2024, 640, pp.123111. 10.1016/j.jnoncrysol.2024.123111 . hal-04636715

HAL Id: hal-04636715

<https://hal.science/hal-04636715v1>

Submitted on 8 Nov 2024

HAL is a multi-disciplinary open access archive for the deposit and dissemination of scientific research documents, whether they are published or not. The documents may come from teaching and research institutions in France or abroad, or from public or private research centers.

L'archive ouverte pluridisciplinaire **HAL**, est destinée au dépôt et à la diffusion de documents scientifiques de niveau recherche, publiés ou non, émanant des établissements d'enseignement et de recherche français ou étrangers, des laboratoires publics ou privés.



Distributed under a Creative Commons Attribution 4.0 International License



Effects of hydrostatic pressure on amorphous chiral materials: Impact on homochiral or heterochiral H-bond sequences

Bienvenu Atawa^{a,b}, Nicolas Couvrat^b, Frédéric Affouard^c, Natália T. Correia^c, Gérard Coquerel^b, Allisson Saiter-Fourcin^{a,*}

^a Univ Rouen Normandie, INSA Rouen Normandie, CNRS, Groupe de Physique des Matériaux UMR 6634, F-76000 Rouen, France

^b Univ Rouen Normandie, SMS, UR 3233, F-76000 Rouen, France

^c Univ Lille, CNRS, INRA, ENSCL, UMR 8207, UMET, Unité Matériaux et Transformations, F59000 Lille, France

ARTICLE INFO

Keywords:
Pressure
BDS
Crystallization
Chirality

ABSTRACT

High pressure effects on static dielectric permittivity of homochiral and heterochiral N-acetyl- α -methylbenzylamine (Nac-MBA) were investigated. For homochiral composition, the static permittivity increases of 178% with pressure at $T = 388$ K. Interestingly, as pressure continued increasing, ϵ_s drastically collapsed to reach $\epsilon_\infty = 3 \pm 0.3$. In the case of heterochiral composition, the static permittivity increases with pressure (in the same magnitude order as the pure enantiomer), and reaches a constant value depending on the isothermal temperature. Thus, the size of the H-bond aggregates is highly pressure sensitive, increasing up to a level that crystallization becomes unavoidable. For heterochiral composition, this process may be kinetically time consuming since the initial heterochiral H-bond aggregates need to be surrounded by their suitable neighbors in order to fulfilled the crystalline packing. The initial H-bond sequences are the precursors of the future crystalline arrangement under pressure application.

1. Introduction

Hydrogen bonding plays an essential role in many biological, chemical and physical processes. One of the most famous examples is the role played by the H-bonding between water molecules. In absence of this bonding, water would not possess some of its genius properties such as its high surface tension, the ability to dissolve many other molecules or to crystallize with gas (Clathrates) and numerous ionic compounds [1, 2]. Structurally speaking, these bonding can lead to supramolecular architectures enhancing typical properties [3]. One of these peculiar behaviors well known in dielectric science is the appearance of high dielectric responses favored by supramolecular structures built from H-bonding [4,5]. This is the case of N-acetyl- α -methylbenzylamine (Nac-MBA) for which the dielectric response of the main process represents almost 90% of the global dielectric permittivity [6]. The main dielectric process appears as a single exponential contribution known as the Debye relaxation. The process is generally associated to the transitory attachment/detachment of H-bond aggregates, leading to supramolecular structures with effective giant dipoles [4,5,7,8]. However, the nature and the architecture of these H-bonds aggregates are not yet fully

clarified [9–11] even though such high magnitude response is consistent with the formation of linear H-bond molecular chains. A modification of these H-bond architectures usually occurs upon temperature variation [4,5,12,13], high pressure [12,14–16] or large electric field applications [10].

A renewed interest on the influence of compression on Debye forming liquids and especially on monohydroxy alcohol family recently appeared in literature [14,17,18]. One critical parameter remains the evolution under pressure of the dielectric response of the Debye relaxation. This evolution is usually linked to the position of the hydroxyl group in the molecule. Whenever the OH group is positioned at the end of the molecule, the formation of linear H-bond chains seems more favored. Under increasing pressure the Kirkwood factor g_K decreases and the dielectric response follows the same behavior. This may suggest that the effective dipole of the aggregate is reduced upon compression. Such behavior is noticed for 2-ethyl-1-hexanol (2E1H) [14,16]. Nonetheless when the OH group is sterically hindered, the formation of ring structures is mostly favored. Under increase pressure, g_K increases (same as the dielectric response of the Debye process) in such a way that the ring structures are converted into linear H-bond chains [14,16]. This

* Corresponding author.

E-mail address: allisson.saiter@univ-rouen.fr (A. Saiter-Fourcin).

<https://doi.org/10.1016/j.jnoncrysol.2024.123111>

Received 26 March 2024; Received in revised form 26 June 2024; Accepted 30 June 2024

Available online 5 July 2024

0022-3093/© 2024 The Author(s). Published by Elsevier B.V. This is an open access article under the CC BY license (<http://creativecommons.org/licenses/by/4.0/>).

behavior is observed in the case of isomeric heptanols [14,16,19] and octanols [19,20]. In some cases, such as 5-methyl-3-heptanol, the dielectric strength increases with pressure, and reaches a saturation value at high pressure. The stated behaviors are linked to the ability of the liquid to form linear or ring H-bond aggregates [14,16].

The present work focuses on the case of Nac-MBA, a chiral secondary amide. Since the Nac-MBA molecule has a single—NH and a single C = O group, the structures are mainly linear HB chains formed of a sequence of the C = O...H—N motif [6,21]. In this situation, the Debye process originates from the transient formation/disruption of linear molecular H-bond chains. In our previous work, it was evidenced that homochiral arrangements (R-R or S-S or R-R-R or S-S-S) are more favorable compared to heterochiral sequences whatever their tacticity (R-S or S-R or R-S-R-S or S-R-S-R) [6]. Nevertheless, the following questions are worthy to be stretched. Are these aggregates sensitive to changes in density enhanced upon hydrostatic compression? Is there a signature of chirality in the amorphous precursors of the future crystalline homochiral or heterochiral structure? In order to tackle this issue, we performed dielectric measurements under isothermal high-pressure conditions. The analyses were carried out for homochiral and heterochiral compositions of Nac-MBA system.

2. Material and methods

2.1. Samples

Optically pure enantiomers (S (-) and R (+)) of Nac-MBA were obtained by acetylation of α -methyl-benzylamine. The synthesis and purification steps were detailed in a previous work [22]. Both S (-) and R (+) pure enantiomers are displayed in Fig. 1. Additionally, from the pure enantiomer, a heterochiral composition was prepared by mixing both enantiomers in such a way to obtain an enantiomeric excess (ee) of 33%.

2.2. Broadband dielectric spectroscopy

Prior to measurements, the sample is placed in between two gold plated electrodes mounted in a Teflon ring and sealed in order to avoid linkage and isolate the sample from the silicone oil used as pressure medium. The capacitor is then connected to the electric feed-through and placed in the pressure chamber. The dielectric measurements

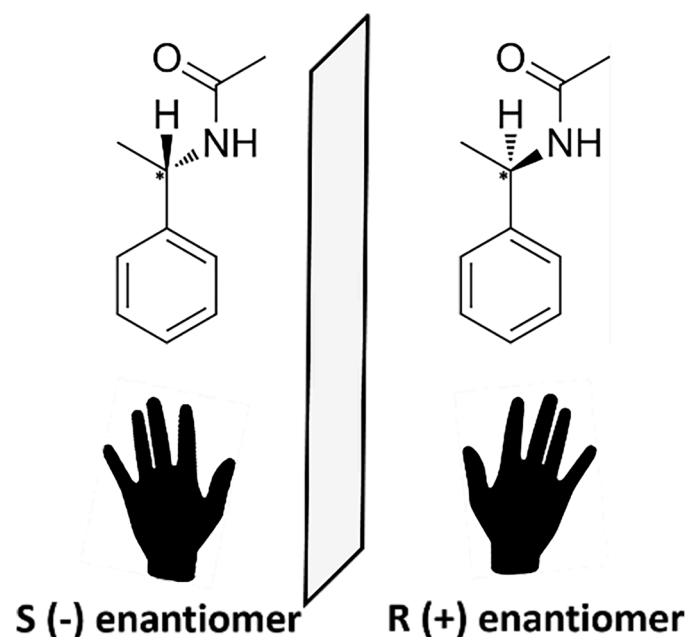


Fig. 1. Schematic representation of S (-) and R (+) Nac-MBA enantiomers.

were performed isothermally using an Alpha-analyzer from Novocontrol for various pressures ranging from 0.1 MPa up to 600 MPa. A schematic illustration of the high pressure dielectric measurements is shown in Fig. 2.

The isothermal conditions were maintained by means of liquid flow provided by a thermostatic bath. Measurements were achieved under isothermal and isobaric conditions for both homochiral and heterochiral compositions. In our previous work, we illustrated that the original size of H-bond aggregates was directly impacted by changing the annealing temperature. We can artificially change the size of the existing aggregates by modifying the annealing temperature. The size of the aggregates decreases when increasing the annealing temperature [21].

The sample is initially melted at 388 K and annealed for 20 min to ensure a complete melting. The binary phase diagram of Nac-MBA at atmosphere pressure suggest that at 388 K, both pure enantiomer and scalemic compositions are in the liquid state [21]. Consequently, the isothermal conditions were chosen in the liquid and supercooled liquid state at atmosphere pressure ($333\text{ K} \leq T \leq 388\text{ K}$) where crystallization did not occur for non-pressurized samples. When necessary, the sample is cooled down to an isothermal temperature and pressurized. An annealing time is necessary to stabilize the temperature. In order to estimate the random and systematic errors, the measurement is repeated for the same temperature and the same pressure at least twice. The same protocol is applied at selected couple (T, P) and for both enantiomeric compositions and the evolution of the real dielectric permittivity is analyzed under pressure condition.

3. Results and discussions

Dielectric spectroscopy on associating liquids measures the effective dipole moment of such assemblies which can be greater or smaller compared to the dipole moment of the single molecule depending on the molecular structure. In dielectric theory ϵ_S is defined as the zero-frequency limit of the real part of the frequency-dependent complex dielectric permittivity. According to the Kirkwood approach, the dielectric constant is directly correlated to the number of dipoles relaxing unit N, the effective dipole moment μ and the orientational correlation factor g_K [23]. According to Fröhlich and Kirkwood approach ϵ_S is given by the following equation:

$$\epsilon_S = \frac{1}{3\epsilon_0} F g_K \frac{\mu^2}{k_B T} \frac{N}{V} + \epsilon_\infty \quad (1)$$

Where F is the Onsager factor, μ the permanent dipole moment, N the number of relaxing units in a volume V, k_B the Boltzmann constant, T the temperature of the system, and ϵ_∞ the highest frequency value of the real permittivity.

The evolution of the static permittivity as function of the pressure is evaluated for homo chiral and hetero chiral associations. In the present paper, this parameter is used to evaluate the impact of pressure in the reorganization of the H-bond aggregates.

Figs. 3a) b) and c) show the pressure evolution of the real dielectric permittivity at three selected temperatures a) 343 K b) 363 K and c) 388 K for a sample presenting an homochiral composition. Fig. 3d) illustrates the pressure evolution of the static permittivity at the selected temperatures for the same sample. Prior to pressure application, all the samples were in the supercooled liquid or liquid states.

As pressure increases, the dielectric response shifts towards lower frequencies and consequently the relaxation time increases. This behavior is conventionally observed in glass forming liquids [13,14,16,17,24].

At $T = 343\text{ K}$, the static permittivity ϵ_S increases by 54% from $\epsilon_S=24 \pm 2$ at $P = 0.1\text{ MPa}$ up to $\epsilon_S=37 \pm 4$ at $P = 180\text{ MPa}$. At higher pressure, the permittivity drastically drops to $\epsilon_S=3 \pm 0.3$.

At $T = 363\text{ K}$, the static permittivity ϵ_S increases by 87% from $\epsilon_S=15 \pm 1$ at $P = 0.1\text{ MPa}$ up to $\epsilon_S=28 \pm 3$ at $P = 180\text{ MPa}$. At higher pressure, the permittivity drastically drops to $\epsilon_S=3 \pm 0.3$.

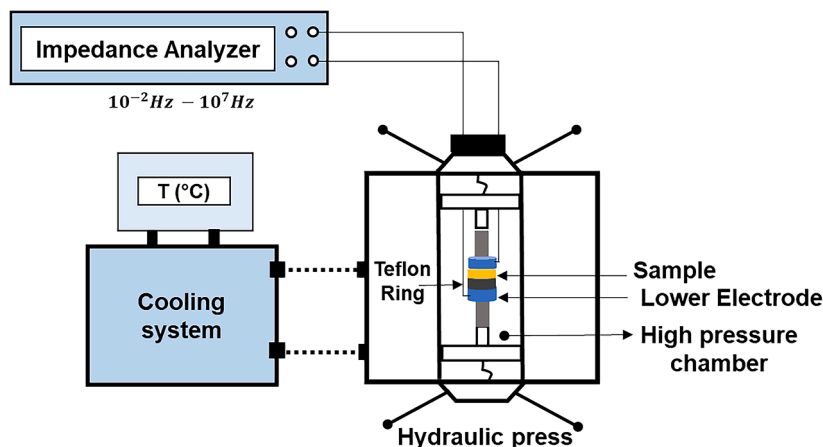


Fig. 2. Schematic illustration of the high-pressure dielectric measurement.

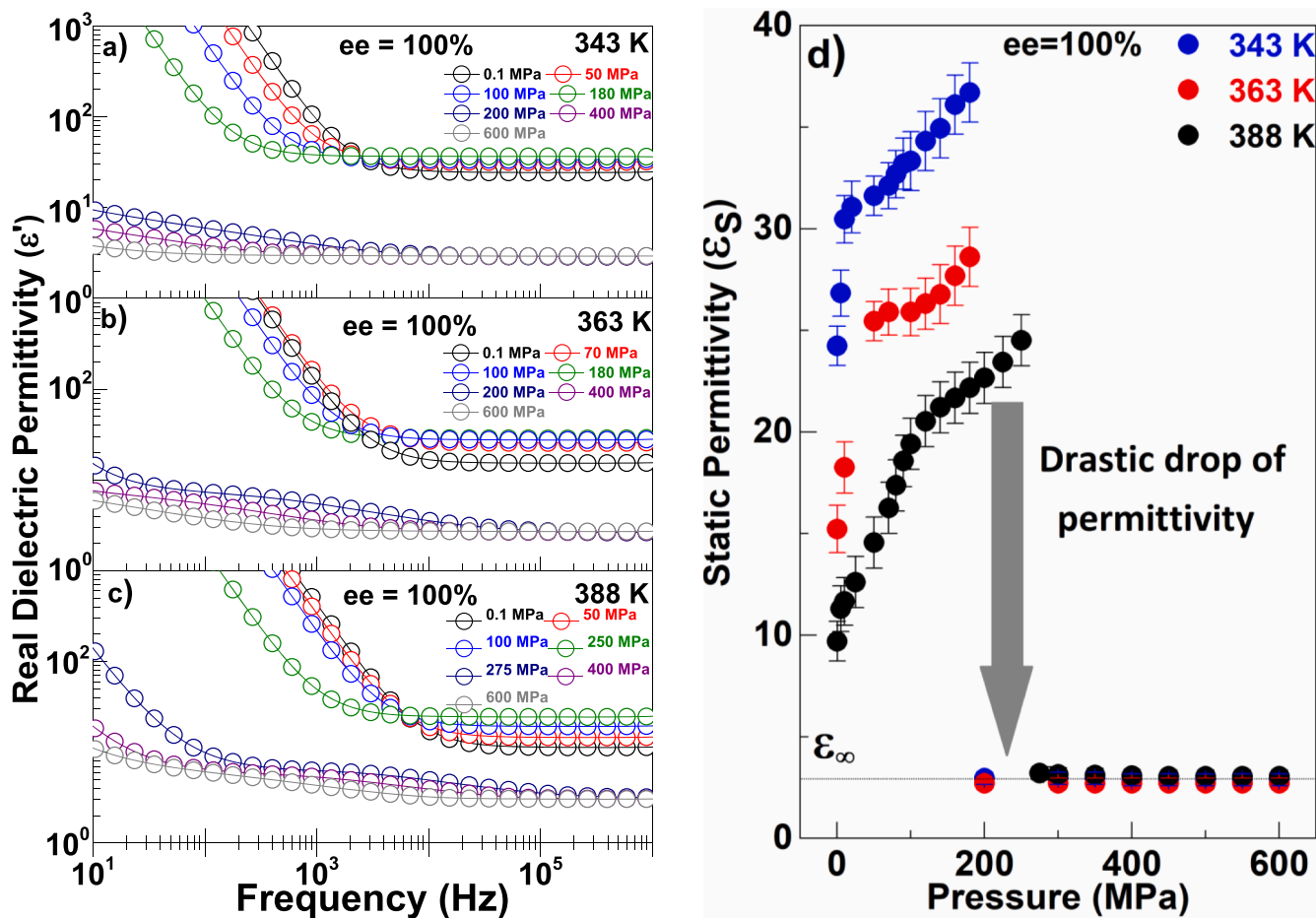


Fig. 3. Pressure evolution of the real permittivity at different temperatures a) $T = 343$ K, b) $T = 363$ K c) $T = 388$ K for a homochiral composition, d) Pressure evolution of the static permittivity at different temperatures for the same homochiral composition.

At $T = 388$ K, the static permittivity ϵ_S increases by 178% from $\epsilon_S = 9 \pm 0.9$ at $P = 0.1$ MPa up to $\epsilon_S = 25 \pm 3$ at $P = 250$ MPa. At higher pressure, the permittivity drastically drops to $\epsilon_S = 3 \pm 0.3$.

Upon compression, the static permittivity increases up to a maximum value and suddenly drops down to $\epsilon_\infty = 3 \pm 0.3$. The increase of the static permittivity is related to the increase of the size of the H-bond aggregates. Likewise, the abrupt faint of the static permittivity is due to the rapid loss of molecular mobility directly imputed to the appearance

of crystals under pressure conditions. Fig. 4 shows a schematic representation of the evolution of linear H-bond chains formed by homochiral sequences (S-S-S or R-R-R) under increasing pressure and the enhancement of crystalline ordering. Upon increasing pressure, the dimension of the aggregates increases up to a critical size where crystallization highly favorable and unavoidable.

The growth kinetics of the aggregates is strongly sensitive to temperature since the static permittivity evolves with temperature under the

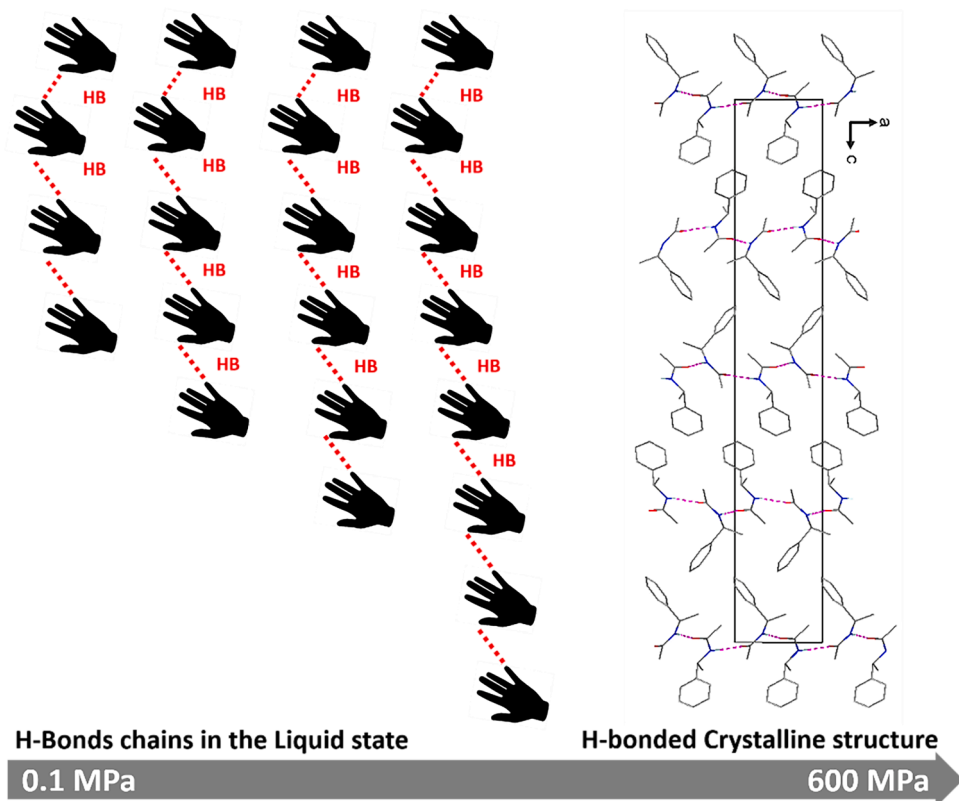


Fig. 4. Schematic illustration of the homochiral H-bonds sequences evolution under increasing pressure in the supercooled liquid ($333\text{ K} \leq T \leq 388\text{ K}$) precursor of the displayed crystalline structure.

same isobaric conditions. For the same isobaric conditions, the static permittivity stays higher at 343 K than at 363 K and 388 K. Moreover, the drop of the static permittivity arises at higher pressure for $T = 388\text{ K}$ compared to $T = 363\text{ K}$ or 343 K. These observations may suggest that the size of H-bond aggregates seems higher at lower temperatures for the same isobaric condition. Thus, the architecture of the aggregates formed at low temperature are closer to the crystalline packing compared to those formed at high temperature since they possess larger homochiral sequences. At $T = 388\text{ K}$, higher pressure conditions are required to obtain the same size of aggregates in order to enhance the crystallization process.

The strong crystallization propensity of the pure enantiomer is not deteriorated by pressure application since crystallization always occurs at high pressure. One may ask about the situation for a sample when containing both enantiomers.

Fig. 5 illustrates the pressure evolution of the real dielectric permittivity at four selected temperatures (a) 333 K, (b) 363 K, (c) 373 K, and (d) 388 K in the available frequency range for a sample with an ee = 33%.

The pressure evolution of the static permittivity at the four temperatures is resumed in Fig. 5(e). As illustrated, the static permittivity possesses a sigmoidal shape. When pressure increases, ϵ_s slowly increases and evolve toward a constant (maximum) value. At low pressure values ($< 200\text{ MPa}$), the static permittivity increases when temperature decreases. Nevertheless, this temperature dependency behavior of the static permittivity disappears at pressure $P > 200\text{ MPa}$.

Under isothermal conditions, the pressure required to reach the maximum static permittivity is temperature dependent. As the isothermal temperature rises, the pressure at the maximum static permittivity increases. For a given isothermal temperature $T = 388\text{ K}$, the static permittivity reaches its maximum value $\epsilon_s = 24 \pm 2$ at $P = 400\text{ MPa}$, while at $T = 333\text{ K}$ the pressure decreases down to 150 MPa when $\epsilon_s = 28 \pm 2$ is at its maximal value. These results may suggest that

pressure increases the effective dipole moment as well as the correlation amongst neighboring molecules. Fig. 6 displays a schematic illustration of the increase of the linear H-bond chains formed by heterochiral sequences upon increasing pressure and the progressive building of the future crystalline structure.

Moreover, upon isothermal compression the number of molecules implicated in the formation of the H-bond aggregates seems to increase. Such situation may structurally lead to a sample with higher density but smaller than that of the crystal. Since the static permittivity is constant after a certain pressure it seems obvious that the architecture and the size of the H-bond aggregates are not modified even for much more important compression. When the static permittivity has reached a saturation value, the H-bond aggregates can no longer grow and the sample stays in the metastable liquid state. These aggregates are therefore precursors of the future crystalline structure but some thermodynamic and kinetic conditions may be fulfilled prior to the beginning of crystallization. For example, each enantiomer must be surrounded by its proper neighbors. Anyway, such process is lazy and time consuming.

Fig. 7 illustrates the time dependency of the static permittivity at the analyzed isothermal temperatures for the highest reachable pressure ($P = 600\text{ MPa}$). The time evolution of the static permittivity shows a sigmoidal shape (for $T = 373\text{ K}$, $T = 388\text{ K}$). For short annealing time, the static permittivity stays briefly at its maximum value and slowly decreases down to the high frequency permittivity as the annealing time increases. When $T = 333\text{ K}$ the static permittivity remains always constant during the isothermal measurements (300 min).

The drop of permittivity at both 373 K and 388 K is hypothetically linked to the loss of molecular mobility associated to crystallization of the supercooled liquid. Under these isobaric and isothermal conditions, crystallization appears much more rapidly at 388 K than 373 K. The static permittivity stays constant at 333 K even for long annealing time (300 min). Therefore, no crystallization can be noticed at that

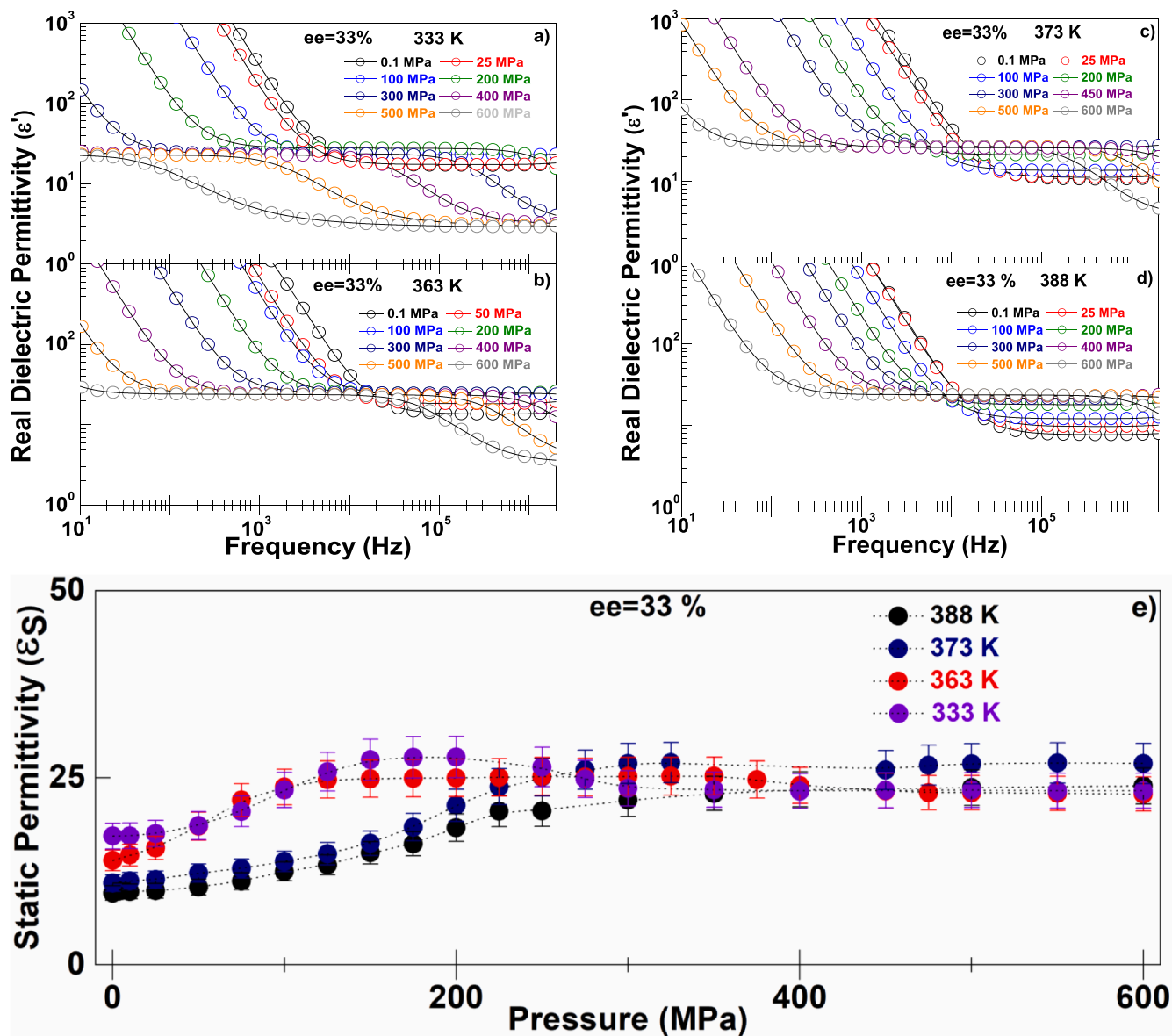


Fig. 5. Pressure evolution of the real dielectric permittivity at a) 333 K b) 363 K c) 373 K and d) 388 K for an heterochiral composition (ee = 33%). e) Pressure evolution of the static permittivity at different temperatures for the same composition.

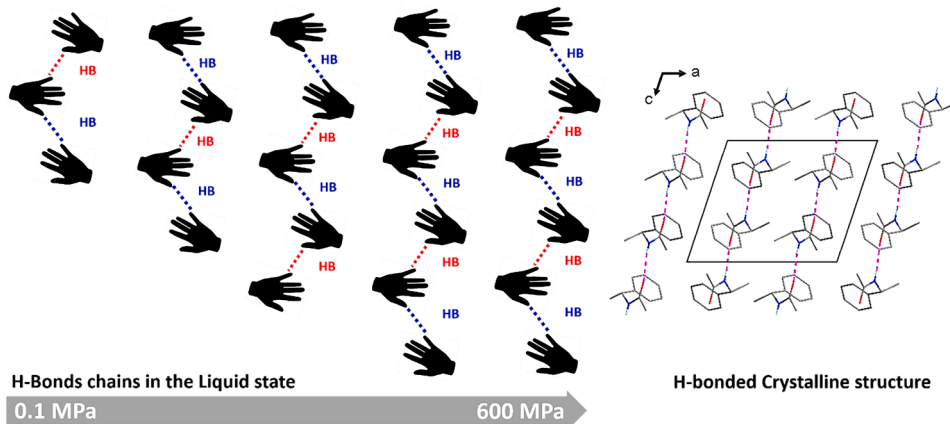


Fig. 6. Schematic illustration of the heterochiral H-bond sequences evolution under increasing pressure in the supercooled liquid ($333\text{ K} \leq T \leq 388\text{ K}$) precursor of the displayed crystalline structure.

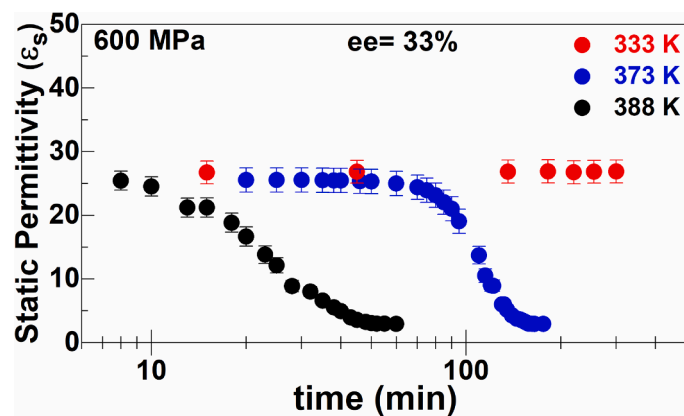


Fig. 7. Time evolution of the static permittivity for a scalemic composition at 600 MPa for different temperatures.

temperature. For crystallization to appear, the growth of the nuclei must occur. The nucleation and growth processes depend on both temperature and pressure conditions. The H-bond aggregates formed at all the analyzed temperatures can be considered as initial “nuclei”. Consequently, nucleation takes place at 333 K, 373 K and 388 K while crystal growth seems to take place above 333 K. The crystalline structure is built by infinite H-bond molecular chains made of alternated enantiomers with opposite chirality [25]. Crystallization seems to be time consuming and lazy at low temperature, but facilitated at elevated temperature since molecular mobility becomes high enough. In these conditions, the alternated opposite enantiomers can easily form infinite H-bond molecular chains upon crystal packing.

When comparing the pressure evolution of the static permittivity at both heterochiral and homochiral compositions, it is obvious that crystallization can easily take place in the latter composition since each enantiomer is directly surrounded by the suitable neighbors (crystallization can be delayed at the heterochiral composition due to the presence of both opposite enantiomers). Thus, linear H-bond aggregates can easily be formed without supplementary kinetic constraints. Pressurization therefore enhances crystallization of the supercooled liquid by promoting the edification of large size H-bond aggregates closely packed with strong similarities regarding the crystalline packing. The crystallization under pressure of the heterochiral system led to heterochiral arrangement in the crystalline structure. At atmospheric pressure, the homochiral crystals are slightly denser (1.14 g/cm^3) compared to their heterochiral counterpart (1.12 g/cm^3). Under high pressure conditions, one can imagine that the volume cell of heterochiral crystals should reduce and evolve towards the density of the homochiral crystals. Collet and coworkers suggested that the occurrence of stable homochiral systems (conglomerates) may increase upon high pressure crystallization of chiral molecules [26]. Mandelic acid for which the homochiral crystals are 2.3% more denser than the heterochiral crystals (racemic compound) at ambient pressure was predicted to evolve towards stable homochiral crystals (conglomerate) at 1200 MPa [26]. For the case of Nac-MBA system, no conversion of the heterochiral arrangements toward homochiral ones was observed under high pressure application in the supercooled liquid state. From our previous work [21], we suggested that Nac-MBA could be classified as an H-bond liquid like system, since the liquid is made of a large variety of H-Bond aggregates ranging from isolated molecule to very large clusters made of 20 molecules. Even though, the most probable aggregates are made of 2, 3 or 4 molecules, there is a strong predisposition in the supercooled or liquid states to build homochiral or heterochiral arrangements independently of pressure application. Through a volume reduction effect, high pressure brings the aggregates closer to each other as well as the isolated molecules. One can assume a decrease of the distance between aggregates/aggregates, aggregates/isolated molecules, isolated

molecules/isolated molecules. In heterochiral composition, the static disorder of the aggregates in the liquid or supercooled liquid highly slows down the crystallization kinetics in comparison to an homochiral composition. It is therefore energetically more favorable to build heterochiral entities than to destroy them and rebuild homochiral arrangements. This may explain why under pressure crystallization, the heterochiral composition evolves towards heterochiral crystalline arrangement.

4. Conclusion

Pressure application on heterochiral and homochiral compositions of Nac-MBA system seems to increase the size of the existing linear H-bond aggregates in as much as the static permittivity increases with pressure in both compositions before the occurrence of crystallization. The aggregates formed at a heterochiral composition rapidly reach the same constant and maximum size at different pressure and temperature conditions. The lower the investigated temperature, the lower the pressure will be required to reach the maximum size of these aggregates. This saturation behavior may be linked to the fact that the aggregates are formed by alternated opposite enantiomers. Actually, the counter enantiomers act like an impurity of the same chemical nature that may disturb the establishment of bigger size H-bond molecular chains. However, compression promotes closely packed linear H-bond aggregate structure and enhances crystallization. These H-bond aggregates are therefore precursors of the future crystalline packing (infinite H-bond molecular chains made of opposite enantiomers). The same conclusion can be made for homochiral composition since crystallization is preceded by a strong increase of the H-bond aggregates size upon compression. Pressurization accelerates crystallization of the homochiral supercooled liquid (in comparison to the heterochiral one), forasmuch as the liquid contain molecules of the same chirality. This situation may promote the establishment of infinite H-bond molecular chains made of identical enantiomers. Therefore, the future crystalline structure is strongly sensitive to the homochiral and heterochiral H-bond sequences existing in the supercooled liquid state.

CRediT authorship contribution statement

Bienvenu Atawa: Writing – original draft, Validation, Methodology, Investigation, Formal analysis, Data curation, Conceptualization. **Nicolas Couvrat:** Writing – review & editing, Validation, Supervision, Project administration, Funding acquisition. **Frédéric Affouard:** Validation, Methodology. **Natália T. Correia:** Validation, Methodology. **Gérard Coquerel:** Validation, Funding acquisition. **Allisson Saiter-Fourcin:** Writing – review & editing, Validation, Supervision, Resources, Project administration, Funding acquisition.

Declaration of competing interest

The authors declare that they have no known competing financial interests or personal relationships that could have appeared to influence the work reported in this paper.

Data availability

Data will be made available on request.

Acknowledgement

The authors are grateful to FEDER and Region Normandie for the financial support of this work through the Feder MACHI project.

References

- [1] G.A. Jeffrey, W. Saenger, *Hydrogen Bonding in Biological Structures*, Springer Science & Business Media, 2012.
- [2] E. Brini, C.J. Fennell, M. Fernandez-Serra, B. Hribar-Lee, M. Lukšič, K.A. Dill, How Water's Properties Are Encoded in Its Molecular Structure and Energies, *Chem. Rev.* 117 (2017) 12385–12414, <https://doi.org/10.1021/acs.chemrev.7b00259>.
- [3] J. Uchida, M. Yoshio, T. Kato, Self-healing and shape memory functions exhibited by supramolecular liquid-crystalline networks formed by combination of hydrogen bonding interactions and coordination bonding, *Chem. Sci.* 12 (2021) 6091–6098, <https://doi.org/10.1039/D0SC06676A>.
- [4] R. Böhmer, C. Gainaru, R. Richert, Structure and dynamics of monohydroxy alcohols—Milestones towards their microscopic understanding, 100 years after Debye, *Phys. Rep.* 545 (2014) 125–195, <https://doi.org/10.1016/j.physrep.2014.07.005>.
- [5] S.P. Bierwirth, J. Bolle, S. Bauer, C. Sternemann, C. Gainaru, M. Tolan, R. Böhmer, Scaling of Suprastructure and Dynamics in Pure and Mixed Debye Liquids, in: F. Kremer, A. Loidl (Eds.), *Scaling Relax. Process*, Springer International Publishing, Cham, 2018, pp. 121–171, https://doi.org/10.1007/978-3-319-72706-6_5.
- [6] B. Atawa, N.T. Correia, N. Couvrat, F. Affouard, G. Coquerel, E. Dargent, A. Saiter, Molecular mobility of amorphous N-acetyl- α -methylbenzylamine and Debye relaxation evidenced by dielectric relaxation spectroscopy and molecular dynamics simulations, *Phys. Chem. Chem. Phys.* 21 (2019) 702–717, <https://doi.org/10.1039/C8CP04880K>.
- [7] S.P. Bierwirth, G. Honorio, C. Gainaru, R. Böhmer, Linear and nonlinear shear studies reveal supramolecular responses in supercooled monohydroxy alcohols with faint dielectric signatures, *J. Chem. Phys.* 150 (2019) 104501, <https://doi.org/10.1063/1.5086529>.
- [8] G. Honorio, S.P. Bierwirth, C. Gainaru, R. Böhmer, Nonlinear electrical and rheological spectroscopies identify structural and supramolecular relaxations in a model peptide, *Soft Matter* 15 (2019) 4334–4345, <https://doi.org/10.1039/C9SM00434C>.
- [9] L. Zoranić, F. Sokolić, A. Perera, Microstructure of neat alcohols: a molecular dynamics study, *J. Chem. Phys.* 127 (2007) 024502, <https://doi.org/10.1063/1.2753482>.
- [10] L.P. Singh, R. Richert, Watching Hydrogen-Bonded Structures in an Alcohol Convert from Rings to Chains, *Phys. Rev. Lett.* 109 (2012) 167802, <https://doi.org/10.1103/PhysRevLett.109.167802>.
- [11] L.P. Singh, C. Alba-Simionesco, R. Richert, Dynamics of glass-forming liquids. XVII. Dielectric relaxation and intermolecular association in a series of isomeric octyl alcohols, *J. Chem. Phys.* 139 (2013) 144503, <https://doi.org/10.1063/1.4823998>.
- [12] S. Pawlus, M. Paluch, M. Nagaraj, J.K. Vij, Effect of high hydrostatic pressure on the dielectric relaxation in a non-crystallizable monohydroxy alcohol in its supercooled liquid and glassy states, *J. Chem. Phys.* 135 (2011) 084507, <https://doi.org/10.1063/1.3626027>.
- [13] K. Grzybowska, M. Paluch, A. Grzybowski, S. Pawlus, S. Ancherbak, D. Prevosto, S. Capaccioli, Dynamic Crossover of Water Relaxation in Aqueous Mixtures: effect of Pressure, *J. Phys. Chem. Lett.* 1 (2010) 1170–1175, <https://doi.org/10.1021/jz100154u>.
- [14] C. Gainaru, M. Wikarek, S. Pawlus, M. Paluch, R. Figuli, M. Wilhelm, T. Hecksher, B. Jakobsen, J.C. Dyre, R. Böhmer, Oscillatory shear and high-pressure dielectric study of 5-methyl-3-heptanol, *Colloid Polym. Sci.* 292 (2014) 1913–1921, <https://doi.org/10.1007/s00396-014-3274-0>.
- [15] A. Reiser, G. Kasper, C. Gainaru, R. Böhmer, Communications: high-pressure dielectric scaling study of a monohydroxy alcohol, *J. Chem. Phys.* 132 (2010) 181101, <https://doi.org/10.1063/1.3421555>.
- [16] S. Pawlus, M. Wikarek, C. Gainaru, M. Paluch, R. Böhmer, How do high pressures change the Debye process of 4-methyl-3-heptanol? *J. Chem. Phys.* 139 (2013) 064501 <https://doi.org/10.1063/1.4816364>.
- [17] K.L. Ngai, S. Pawlus, M. Paluch, Explanation of the difference in temperature and pressure dependences of the Debye relaxation and the structural α -relaxation near T_g of monohydroxy alcohols, *Chem. Phys.* 530 (2020) 110617, <https://doi.org/10.1016/j.chemphys.2019.110617>.
- [18] I.V. Danilov, A.A. Pronin, E.L. Gromnitskaya, M.V. Kondrin, A.G. Lyapin, V. V. Brazhkin, Structural and Dielectric Relaxations in Vitreous and Liquid State of Monohydroxy Alcohol at High Pressure, *J. Phys. Chem. B* 121 (2017) 8203–8210, <https://doi.org/10.1021/acs.jpcc.7b05335>.
- [19] J.K. Vij, W.G. Scaife, J.H. Calderwood, The pressure and temperature dependence of the complex permittivity of heptanol isomers, *J. Phys. Appl. Phys.* 14 (1981) 733–746, <https://doi.org/10.1088/0022-3727/14/4/026>.
- [20] G.P. Johari, W. Dannhauser, Effect of Pressure on Dielectric Relaxation in Isomeric Octanols, *J. Chem. Phys.* 50 (1969) 1862–1876, <https://doi.org/10.1063/1.1671282>.
- [21] B. Atawa, N. Couvrat, F. Affouard, N.T. Correia, G. Coquerel, A. Saiter-Fourcin, Impact of chirality on the amorphous state of conglomerate forming systems: a case study of N-acetyl- α -methylbenzylamine, *Phys. Chem. Chem. Phys.* 23 (2021) 24282–24293, <https://doi.org/10.1039/D1CP03843E>.
- [22] B. Atawa, N. Couvrat, G. Coquerel, E. Dargent, A. Saiter, Chirality impact on physical ageing: an original case of a small organic molecule, *Mater. Lett.* 228 (2018) 141–144, <https://doi.org/10.1016/j.matlet.2018.05.133>.
- [23] A. Schönhals, F. Kremer, Theory of Dielectric Relaxation, in: F. Kremer, A. Schönhals (Eds.), *Broadband Dielectr. Spectrosc.*, Springer, Berlin, Heidelberg, 2003, pp. 1–33, https://doi.org/10.1007/978-3-642-56120-7_1.
- [24] J. Trubert, L. Matkovska, A. Saiter-Fourcin, L. Delbreilh, Highlighting the interdependence between volumetric contribution of fragility and cooperativity for polymeric segmental relaxation, *J. Chem. Phys.* 160 (2024) 044909, <https://doi.org/10.1063/5.0187941>.
- [25] S. Druot, N. Petit, S. Petit, G. Coquerel, N. Chanh, Experimental Data and Modelling of the Interactions in Solid State and in Solution between (R) and (S) N-Acetyl- α -Methylbenzylamine. Influence on Resolution by Preferential Crystallization, *Mol. Cryst. Liq. Cryst. Technol. Sect. Mol. Cryst. Liq. Cryst.* 275 (1996) 271, <https://doi.org/10.1080/10587259608034081>.
- [26] A. Collet, L. Ziminski, C. Garcia, F. Vigné-Maeder, Chiral Discrimination in Crystalline Enantiomer Systems: facts, Interpretations, and Speculations, in: J. S. Siegel (Ed.), *Supramol. Stereochem*, Springer Netherlands, Dordrecht, 1995, pp. 91–110, https://doi.org/10.1007/978-94-011-0353-4_12.